

Geophysical Research Letters

RESEARCH LETTER

10.1029/2021GL093552

Key Points:

- Epidote (Ep) and chlorite (Cl) are two low-grade metamorphic minerals typically present in geothermal reservoirs
- Fault instability is promoted by Ep-rich gouges at hydrothermal conditions but minimized with the addition of Cl
- Interplay of Ep/Cl mixtures exerts a detectable control on fault strength and stability for geothermal reservoirs

Supporting Information:

Supporting Information may be found in the online version of this article.

Correspondence to:

F. Zhang,
fengshou.zhang@tongji.edu.cn

Citation:

An, M., Zhang, F., Min, K.-B., Elsworth, D., Marone, C., & He, C. (2021). The potential for low-grade metamorphism to facilitate fault instability in a geothermal reservoir. *Geophysical Research Letters*, 48, e2021GL093552. <https://doi.org/10.1029/2021GL093552>

Received 26 MAR 2021

Accepted 22 MAY 2021

The Potential for Low-Grade Metamorphism to Facilitate Fault Instability in a Geothermal Reservoir

Mengke An^{1,2}, Fengshou Zhang^{1,2} , Ki-Bok Min³ , Derek Elsworth^{4,5} , Chris Marone^{5,6} , and Changrong He⁷ 

¹Department of Geotechnical Engineering, College of Civil Engineering, Tongji University, Shanghai, China, ²Key Laboratory of Geotechnical & Underground Engineering of Ministry of Education, Tongji University, Shanghai, China, ³Department of Energy Resources Engineering and Research Institute of Energy and Resources, College of Engineering, Seoul National University, Seoul, Republic of Korea, ⁴Department of Energy and Mineral Engineering, EMS Energy Institute and G3 Center, the Pennsylvania State University, PA, USA, ⁵Department of Geosciences, the Pennsylvania State University, PA, USA, ⁶Dipartimento di Scienze della Terra, La Sapienza Università di Roma, Italy, ⁷State Key Laboratory of Earthquake Dynamics, Institute of Geology, China Earthquake Administration, Beijing, China

Abstract Native and fluid circulation-induced metamorphic products may affect the stability of faults in geothermal reservoirs—particularly epidote (Ep) and chlorite (Cl). Our laboratory experiments conducted at hydrothermal conditions show that these two minerals, when precipitated on natural faults, may promote fault instability or failure under conditions typifying a geothermal reservoir. Shear experiments on Ep-rich fault gouges indicate potentially unstable frictional behavior—more pronounced at elevated temperatures and pore fluid pressures—and indicate increased potential for the nucleation of slip instability relative to that of the host granodiorite gouge. Experimental results indicate in particular that Ep can increase the potential for induced seismicity on existing faults. Increased proportions of Cl in gouges stabilize the faults but apparently lower the frictional strength. Our results reveal that the metamorphic minerals exert a subtle but potentially significant control on fault strength and stability in geothermal reservoirs.

Plain Language Summary Fluid injection into EGS (enhanced geothermal systems) reservoirs can reactivate subsurface faults and trigger earthquakes. To understand the influence of fluid injection to earthquake triggering on deep faults we analyzed the frictional properties of simulated faults containing the alteration minerals epidote (Ep) and chlorite (Cl). Many geothermal reservoirs worldwide contain these minerals both natively and as a natural result of water circulation into the hot and reactive reservoir. Our measurements of shear strength and frictional stability at in-situ conditions of such geothermal reservoirs show that the simulated Ep fault gouge may destabilize fault slip at both in-situ conditions and at higher temperatures and pore fluid pressures. The addition of Cl shows the opposite effect, stabilizing the fault and lowering the frictional strength; hence indicating a strong dependence of fault strength and stability on fault zone composition. Our results highlight the importance of natural metamorphism and mineral transformation in controlling fault strength and stability and the potential for earthquake triggering.

1. Introduction

High-pressure fluid injection at an enhanced geothermal system (EGS) site can reactivate critically-stressed faults and trigger earthquakes (Kim et al., 2018; Majer et al., 2007). For a pre-existing mature fault, the fault movement and seismic potential are closely associated with the frictional response of fault gouge (Ikari et al., 2011; Niemeijer & Collettini, 2014). Therefore, a careful understanding of the deep fault/fracture properties and triggered earthquake physics is necessary for assessing and mitigating injection-induced seismic risks (Elsworth, 2013; Lee, et al., 2019a). A direct and reliable way to evaluate deep fault/fracture properties is through experiments on materials at *in-situ* pressure and temperature conditions of the system of interest.

The 2017 M_w 5.5 Pohang earthquake in South Korea is the largest known induced earthquake at an EGS site (Grigoli et al., 2018). Natural fractures recovered from granodiorite (Gra) cores prior to stimulation (enhancement of reservoir permeability by fluid injection) at a depth of 4.2 km in the Pohang geothermal

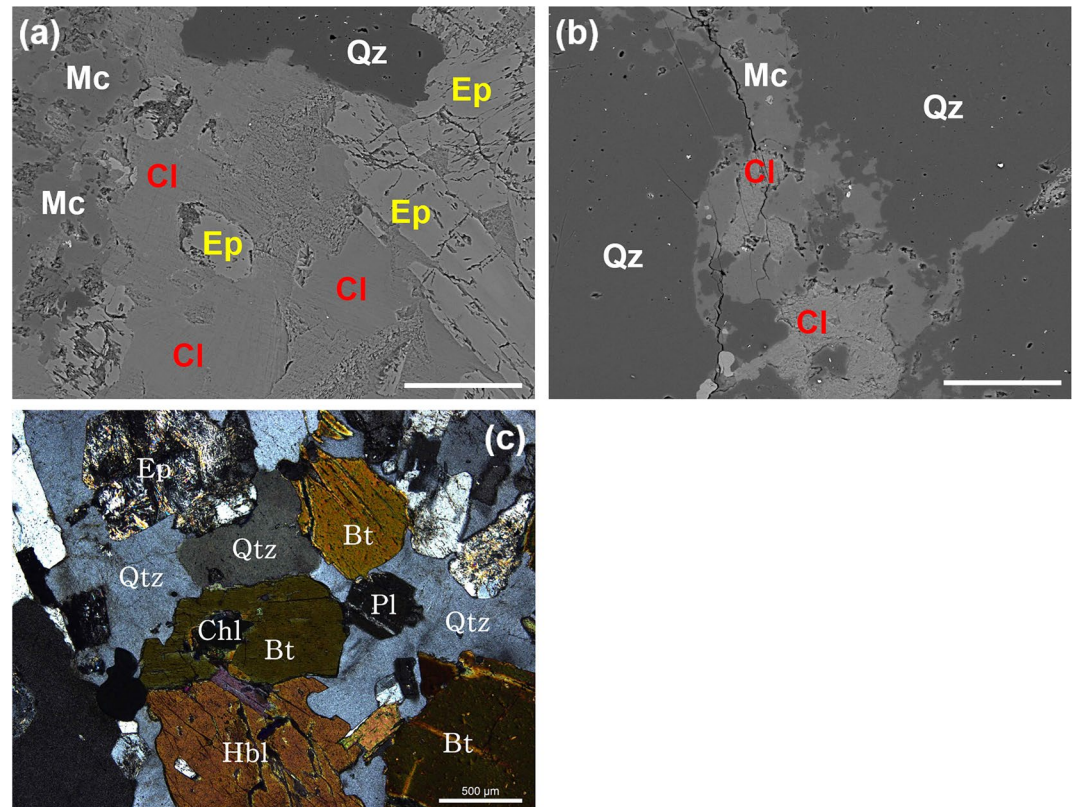


Figure 1. (a) Epidote (Ep) and chlorite occurrences on natural granodiorite (Gra) fractures prior to stimulation from Pohang geothermal site (backscattered electron SEM images) at 4.2 km depth. Native presence of epidote and chlorite (Cl) on the Gra fractures. Other minerals include quartz and microcline. (b) Cl forming at the microcracks of natural Gra cores in Pohang. Scale bars in (a) and (b), 50 μm . (c) Ep and Cl observed in an outcrop sample from the Gonghe geothermal site, China (optical thin section). Scale bar in (c), 500 μm .

reservoir show evidence of alteration on the fracture surface and the native presence of both epidote (Ep) and chlorite (Cl) (Figures 1 and S1). Microstructural characterization and X-ray diffraction analyses indicate the occurrence of epidotization and chloritization along the natural fracture surfaces (Figures 1 and S2). In addition, the borehole cuttings at depths between 3,500 and 3,800 m also contain up to 20 wt% chlorite (Lee et al., 2019b), which is consistent with previous works showing that Ep and Cl are common metamorphic minerals within geothermal systems (Bird & Spieler, 2004; Kwon et al., 2019). The Cl-Ep assemblages are likely to be related to the geological history of the Pohang geothermal site. During the Cretaceous period, low-angle subduction of hot oceanic lithosphere resulted in regional hydrothermal mineralization (Westaway & Burnside, 2019) and the deposition of chlorite and epidote in natural granite fractures (Sarkar et al., 2020; Wehrens et al., 2016). Outcrop samples of granite obtained from the Gonghe geothermal site in China also show the presence of Ep and Cl as shown in Figure 1c. The presence of both Ep and Cl have been reported in numerous geothermal reservoirs including, but not limited to, Soultz (France), Newberry volcano and Coso (USA) (Kovac et al., 2005; Sonnenthal et al., 2012; Vidal & Genter, 2018). Ep is present at 100°C – 200°C within the Onikobe geothermal system (Japan) and at ~200°C in the Sumikaw-Ohnuma (Japan) and Philippine geothermal systems (Bird & Spieler, 2004). Thus, a key question arises as to how these ubiquitous minerals, which are produced as a result of greenschist facies alteration or metamorphism and precipitated as a thin layer on the fault surface, influence fault strength and frictional stability.

To date, few laboratory studies have been carried out to explore the frictional properties of Ep or Cl gouges at hydrothermal conditions (Fagereng & Ikari, 2020; Okamoto et al., 2019). Ep is a nesosilicate mineral that is commonly found in active geothermal systems and volcanic rocks (Bird & Spieler, 2004; Evans, 1990). It is stable over a wide range of temperatures and pressures (<200–700°C, up to 10 kbar), even in subduction zones (Apted & Liou, 1983; Poli & Schmidt, 2004). In addition to being a major rock forming mineral, Ep is

also abundant in veins and distributed within metamorphic, igneous and hydrothermally altered rocks—identifying that metamorphism and fluid-rock interaction can contribute to its presence and abundance (Franz & Liebscher, 2004; Hamilton et al., 2021). At room temperature, the epidote-rich gouges are frictionally strong and exhibit velocity-weakening behavior (Fagereng & Ikari, 2020). Cl is a phyllosilicate mineral found commonly in natural fault zones (Lacroix et al., 2012; Schleicher et al., 2012). Like most phyllosilicate minerals, the sheet structure of Cl exhibits lower frictional strength than tectosilicate or carbonate materials and promotes fault creep (Ikari et al., 2009; Okamoto et al., 2019; Wojatschke et al., 2016). Both Ep and Cl are low-grade metamorphic minerals and they typically coexist in Gra-granite rocks (Poli & Schmidt, 2004). Furthermore, the interplay of the different responses of Ep and Cl will further increase the complexity of fault frictional behavior. Here, we document the effects of temperature, pore fluid pressure and mineral composition on the frictional properties of simulated fault gouges containing Ep and Cl. We report results of laboratory shear experiments at stress conditions corresponding to the 4–5 km depth of a typical geothermal reservoir and different temperatures.

2. Material and Methods

We collected epidote minerals from Handan, Hebei Province of China and chlorite minerals from Fanshi, Shanxi Province of China. Pohang granodiorite (Gra) was recovered from rock cores at a depth of ~4.2 km (Kwon et al., 2019) and only a few hundred meters from the fault that hosted the Pohang earthquake. After removing impurities, samples of Ep and Cl minerals and the native Pohang Gra were crushed and sieved to particle sizes $<75\ \mu\text{m}$ to represent the particles found in the natural fault gouge. Laser particle size analyses identify median particle sizes of the Ep and Cl gouges as 48.7 and 50.3 μm (Figure S3), respectively. X-ray diffraction indicates that both the Ep and Cl gouges have $>99\ \text{wt.}\%$ purity (Figure S4). Ep/Cl mixed gouges were then prepared from the parent minerals in different proportions by weight. The gouge synthesized from crushing of the native Pohang Gra consists of 33 wt.% quartz, 47 wt.% albite, 8 wt.% microcline, 3 wt.% muscovite and 9 wt.% chlorite (Figure S5).

Shear experiments were performed using an argon gas confined triaxial shearing apparatus (Figure S6). A 1 mm thick layer of gouge was sandwiched between the 20 mm diameter gabbro or porous ceramic cylindrical blocks along rough surfaces inclined at 35° to the principal loading axis. The surfaces of these simulated fault zones were roughened with 200-mesh silicon carbide polishing compound. We drilled boreholes into the upper gabbro driving block to apply pore fluid pressures to the fault zone. A brass filter was placed into the borehole at the edge of the fault zone to prevent gouge extrusion and maintain high permeability. The upper porous ceramic driving block was not drilled with a borehole due to its high permeability. In each case, the cylindrical samples and fault zones were inserted into a 0.35 mm thick annealed copper jacket and discs of high-hardness corundum and tungsten carbide blocks were placed at the top and bottom of the cylinders within the copper jacket. At the initiation of the experiment, the confining pressure was applied by the argon gas through a servo-controlled intensifier. Then, the pore fluid (deionized water) pressure was elevated to the desired magnitude, followed by heating of a clamshell furnace to raise the temperature at a rate of $5^\circ\text{C}/\text{min}$. The temperature was maintained constant within $\pm 2^\circ\text{C}$ by an independent controller throughout each experiment.

A confining pressure (σ_c) of 110 MPa and pore fluid pressure (P_f) of 42 MPa were employed, corresponding to lithostatic pressure (with rock density of $2,630\ \text{kg}/\text{m}^3$) and hydrostatic pressure at 4.2 km depth. According to Westaway & Burnside (2019), the temperature at a depth of 2,250 m at the Pohang geothermal site is 103°C and the temperature gradient in the Pohang granite is $28^\circ\text{C}/\text{km}$. The estimated temperature at 4.2 km is therefore $\sim 153^\circ\text{C}$. We explored the frictional properties of epidote gouge at $\sigma_c = 110\ \text{MPa}$, $T = 100^\circ\text{C} - 250^\circ\text{C}$ (temperature) and $P_f = 42 - 63\ \text{MPa}$ and the crushed Pohang Gra gouge at $\sigma_c = 110\ \text{MPa}$, $T = 150^\circ\text{C}$ and $P_f = 42 - 63\ \text{MPa}$. The lower limit of pore fluid pressure ($P_f = 42\ \text{MPa}$) corresponds to the hydrostat and the higher value ($P_f = 63\ \text{MPa}$) accommodates the injection over-pressure. For experiments with mixed Ep/Cl gouges, we varied the chlorite content from 0 to 100 wt.% and gouge states from homogeneously mixed to layered at $\sigma_c = 110\ \text{MPa}$, $T = 150^\circ\text{C}$ and $P_f = 42\ \text{MPa}$. Details are given in Table S1. Each experiment was initially sheared at a constant shear velocity of $1.22\ \mu\text{m}/\text{s}$ until the steady state friction regime was achieved. Then the shear velocity was stepped between 1.22, 0.244 and $0.0488\ \mu\text{m}/\text{s}$ to assess the velocity dependence of friction.

The measured raw force data from the experiments are corrected for the variation in shear-overlap area with increasing shear displacement and the shear resistance of the sealing copper jacket following the methods (Text S1) of He et al. (2006) and Verberne et al. (2010). The coefficient of friction is calculated as $\mu = \tau/(\sigma_n - P_f)$, where τ and σ_n denote the shear stress and normal stress, respectively. Due to the reported pore fluid pressure deviating from a far-field measurement, the calculated coefficients of friction here are apparent coefficients of friction. The velocity dependence was evaluated based on the rate and state friction equation with the Dieterich evolution law (Dieterich, 1979; Rice, 1983; Ruina, 1983), expressed as,

$$\mu = \mu_0 + a \ln\left(\frac{V}{V_0}\right) + b \ln\left(\frac{V_0 \theta}{D_c}\right) \quad (1)$$

$$\frac{d\theta}{dt} = 1 - \frac{V\theta}{D_c} \quad (2)$$

where μ is the coefficient of friction at the instantaneous shear velocity V , μ_0 denotes the coefficient of friction at the reference shear velocity V_0 ($V > V_0$), a and b are dimensionless constants, θ is a state variable that describes contact age and fault zone porosity (Marone, 1998), D_c represents the critical slip distance, and t is time. At a steady state friction, the state variable θ does not change with time t and thus $d\theta/dt = 0$. Then, the frictional stability parameter ($a-b$) can be obtained from Equation 1,

$$a - b = \frac{\mu - \mu_0}{\ln(V/V_0)} = \frac{\Delta\mu}{\Delta \ln V} \quad (3)$$

Negative values of ($a-b$) reveal that the coefficient of friction decreases with an increase of shear velocity (velocity-weakening), promoting potentially unstable frictional sliding. Conversely, positive values of ($a-b$) indicate velocity-strengthening and result in inherently stable sliding. Examples of methods for determining the values of $\Delta\mu$ are shown in Figure S7.

After the shear experiments, the deformed gouge samples were first impregnated with resin in a vacuum chamber and then cut into thin sections along the shear direction for microstructural observation using field emission gun scanning electron microscopy (FEG-SEM).

3. Results

A total of thirteen experiments were conducted at varied gouge compositions, temperatures, and pore fluid pressures (Table S1). The friction displacement curves are typical, with a linear increase initially followed by an inelastic yield point and slight slip hardening (Figures S8, S9 and S10). Stick-slips were found for Ep gouge at $T \geq 150^\circ\text{C}$ and the stick-slip amplitude increased with increasing temperature. Ep fault gouge exhibits consistent μ ranging from 0.73 to 0.75 at different temperatures and pore fluid pressures (Figures 2a and 3a, Table S2). Sliding friction of epidote gouges is insensitive to T and P_f in the studied range. Values of μ of Pohang Gra gouge at the two pore fluid pressures (42 and 63 MPa) are similar to the Ep gouge (Figure 3a). Ep/Cl mixed gouges are frictionally weaker ($\mu = 0.35 - 0.66$) (Table S2) than the Ep gouge at $T = 150^\circ\text{C}$ and $P_f = 42 \text{ MPa}$, and values of μ decrease with increasing Cl content (Figure 2b). Pure Cl gouge is the weakest in our experiments ($\mu = 0.35$), in agreement with previous work (Okamoto et al., 2019) but frictionally stronger than several pure phyllosilicate gouges, like the montmorillonite ($\mu \sim 0.13$), illite ($\mu \sim 0.28$) or talc ($\mu \sim 0.20$) gouges (Giorgetti et al., 2015; Tembe et al., 2010).

Results of our velocity step tests to measure the velocity dependence of friction are summarized in Figures 2c, 2d and 3b and Table S2. Epidote gouge exhibits a range of behaviors from velocity-strengthening ($a-b = 0 - 0.0022$) at $T = 100^\circ\text{C}$, to velocity-neutral ($a-b = -0.0021 - 0.0001$) at $T = 125^\circ\text{C}$ and velocity-weakening ($a-b = -0.0073 - -0.0034$) at $T \geq 150^\circ\text{C}$ (Figure 2c), indicating the higher seismic potential at higher temperatures for Gra faults/fractures lined with metamorphic epidote. At $T = 150^\circ\text{C}$ and $\sigma_c = 110 \text{ MPa}$, elevating P_f from 42 MPa ($a - b = -0.0062 - -0.0039$) to 63 MPa ($a-b = -0.0073 - -0.0056$) destabilizes

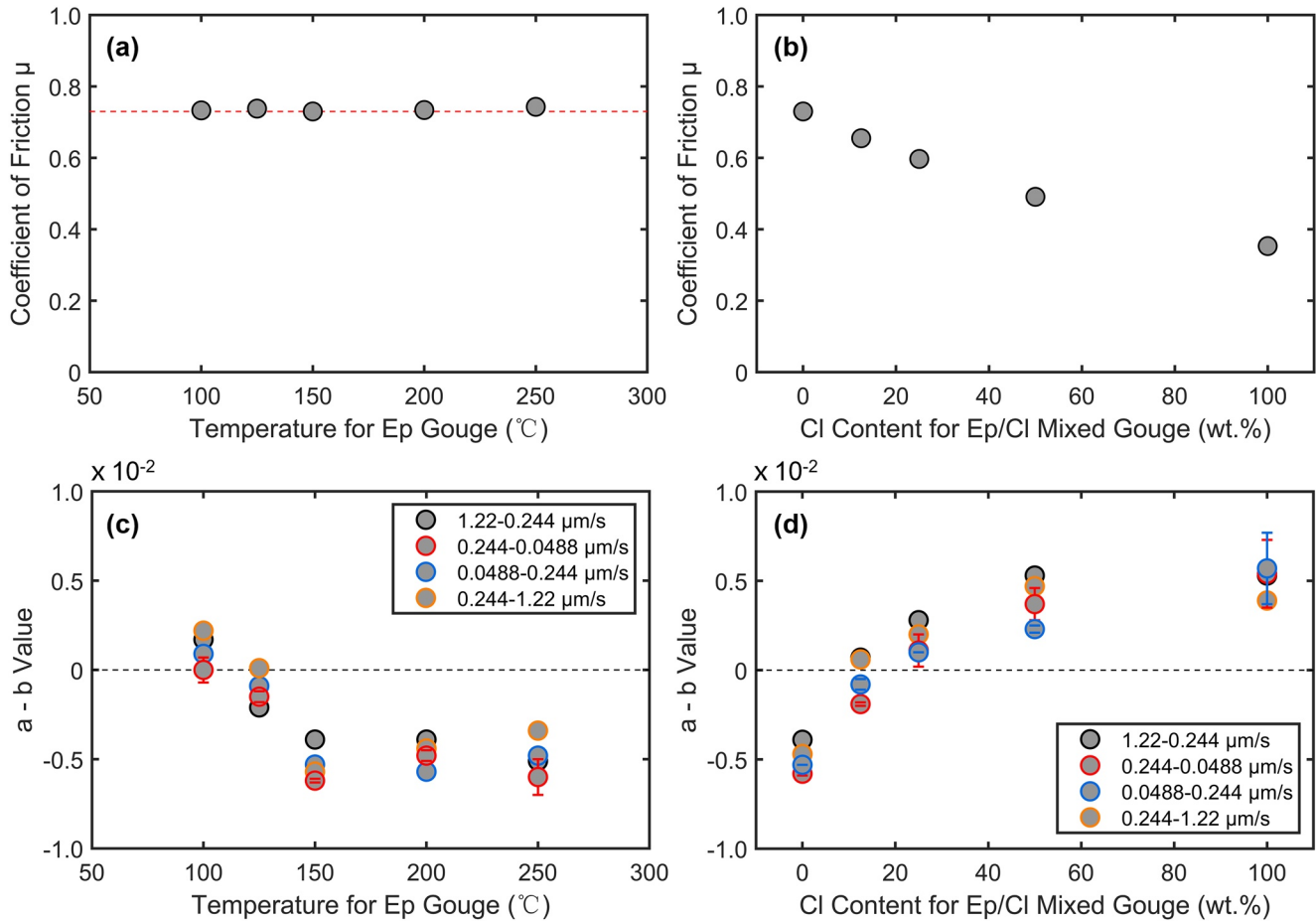


Figure 2. Coefficient of friction μ and frictional stability (a)–(b) for synthetic epidote (Ep) and epidote/chlorite(Cl) mixed gouges at varied conditions. (a) Values of μ versus temperature for Ep gouge at $\sigma_c = 110 \text{ MPa}$ and $P_f = 42 \text{ MPa}$. The red dashed line indicates $\mu = 0.73$. (b) Friction versus Cl content for Ep/Cl gouge at $\sigma_c = 110 \text{ MPa}$, $P_f = 42 \text{ MPa}$ and $T = 150^{\circ}\text{C}$. (c) Friction stability parameter (a)–(b) as a function of temperatures for Ep gouge at $\sigma_c = 110 \text{ MPa}$ and $P_f = 42 \text{ MPa}$. (d) Values of (a)–(b) as a function of the Cl content for Ep/Cl gouges at $\sigma_c = 110 \text{ MPa}$, $P_f = 42 \text{ MPa}$ and $T = 150^{\circ}\text{C}$. The plotted (a)–(b) values are the average values from the same velocity steps in each test with the error calculated from the standard deviation (Table S2).

the epidote gouge (Figure 3b), implying that the variation in pore fluid pressure and effective stress also affects the stability of the Ep gouge. Similar results of fault instability promoted by a decrease in effective stress were reported in Niemeijer and Colletini (2014). The Pohang Gra gouges exhibit velocity-neutral to velocity-weakening behavior ($a-b = -0.0016 - 0.0009$) at $T = 150^{\circ}\text{C}$ and the two pore fluid pressures (42 and 63 MPa) (Figure 3b), in contrast to the work of Blanpied et al. (1991) where the granite gouge shows only velocity-weakening behavior at this temperature. Ep/Cl mixed gouges show velocity-strengthening behavior ($a-b = 0.0010 - 0.0057$) with chlorite content $\geq 25 \text{ wt.}\%$ at $T = 150^{\circ}\text{C}$ and $P_f = 42 \text{ MPa}$, but exhibit velocity-neutral to velocity-weakening behavior ($a-b = -0.0019 - 0.0007$) at $< 25 \text{ wt.}\%$ chlorite content.

Microstructural observations indicate that the Ep-rich gouge samples develop localized shear zones (LSZs) with apparent particle size reduction (Logan et al., 1992) (Figures S11 and S12d). In these LSZ, most Ep particles have diameters $< 30 \mu\text{m}$ due to shear-based comminution, while the epidote particles beyond this zone are less comminuted and retain larger diameters (Figure S11). In contrast, less obvious LSZ, foliations, or fractures are found in the deformed Cl-rich gouge samples (Figures S12a–S12c, Figure S14). For those samples, the Ep particles are surrounded by the layered-structural chlorite particles. Shear is homogeneously distributed throughout the gouge with elongated lamellae of Ep and Cl. The diameters of several elongated Ep particles aligned parallel to the shear direction even reach $> 100 \mu\text{m}$ (Figures S12b and S12c). For the 50% Ep + 50% Cl mixed gouge with layered structure, we observe that the shear mainly develops within the Cl (Figure S12e). Consequently, the value of μ of the layered gouge (50% Ep + 50% Cl) ($\mu = 0.36$) is much

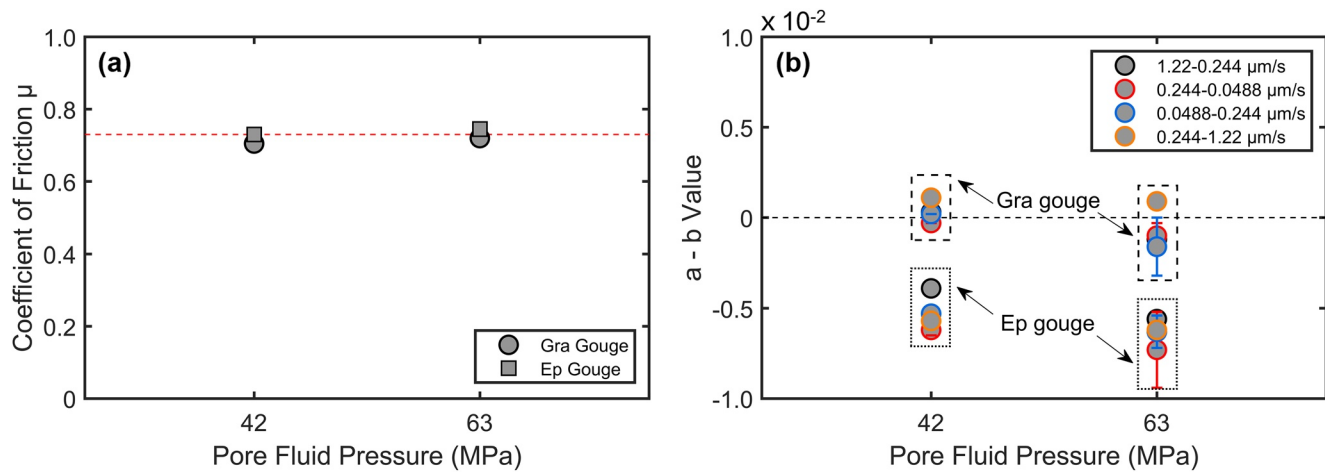


Figure 3. Comparison of (a) coefficient of friction μ and (b) friction stability parameter (a)–(b) for the Pohang granodiorite (Gra) gouge and epidote (Ep) gouge at $\sigma_c = 110$ MPa, $T = 150^\circ\text{C}$ and P_f of 42 and 63 MPa. The red dashed line in (a) indicates $\mu = 0.73$. Note that the Ep gouge is more velocity-weakening than the Pohang Gra gouge. The plotted (a)–(b) values are the average values from the same velocity steps in each test with the error calculated from the standard deviation (Table S2).

lower than that of the homogeneously mixed gouge (50% Ep + 50% Cl) ($\mu = 0.49$), but similar to that of pure chlorite ($\mu = 0.35$) (Figure S13, Table S2). This also supports the observation that the gouge fabric can have a significant effect on gouge friction and that the weak mineral (chlorite) dominates the frictional response of layered gouge (Niemeijer et al., 2010).

4. Discussion

Although both Ep and Cl are low-grade metamorphic minerals, their frictional strength and stability are vastly different. Under hydrothermal conditions, Ep gouge is frictionally strong ($\mu \sim 0.73$) and exhibits velocity-weakening at $T \geq 125^\circ\text{C}$ (Figure 2). Compared to the Pohang Gra gouge (Figure 3), frictional instability is more pronounced in the Ep gouge—indicating a higher potential for instability in the synthetic Ep sample. Conversely, chlorite gouge is frictionally weak ($\mu \sim 0.35$) and promotes only velocity-strengthening behavior (Figure 2). These frictional characteristics are generally consistent with previous results and highlight the role played by mineral structure in fault friction (Bos & Spiers, 2002; Okamoto et al., 2019) (Figure S14).

The transition towards unstable slip ($a-b < 0$) at higher temperatures (Figure 2c) in Ep gouge can be partially explained by a microphysical model for quartz-illite gouges or for carbonate gouges (Chen et al., 2015; Den Hartog & Spiers, 2013; Verberne et al., 2015). This model links shear-induced dilation and its enhancement by pressure solution-induced compaction at higher temperatures to the temperature—and rate-dependence of stability. At higher temperatures, a denser gouge structure forms as a result of gouge compaction by pressure solution and promotes gouge dilation during velocity up-steps. This gouge dilation is stronger than the compaction following the velocity up step and leads to a decrease in frictional strength and thus to velocity-weakening behavior. Besides, the slip stability of both the epidote and Pohang Gra gouges is also apparently influenced by the magnitude of pore fluid pressure. From Faulkner et al. (2018), the potential for instability in low-permeability gouges is promoted when the pore fluid pressure is not given sufficient time to equilibrate. This implies that pore fluid pressures can impact frictional response as a result of different equilibration times.

Our data indicate that homogeneously mixed gouges of epidote/chlorite exhibit velocity-weakening with <25 wt.% Cl at conditions expected for a geothermal reservoir at a depth of 4 – 5 km (Figure 2d). We interpret this to indicate that the presence of epidote in fault gouge and along fracture surfaces can promote unstable slip and earthquakes. Where fractures and faults show the coexistence of Ep and Cl (Figure S1), an important question remains as to whether the Ep or the Cl dominates the mineralogical composition of granitoid gouges and how these relative proportions contribute to frictional instability. Although the

X-ray diffraction results on natural Gra fractures (Figure S2) show a higher content of Ep, the exact mineral composition at the main fault where the M_w 5.5 Pohang earthquake occurred is unknown as it is a few hundred meters away from the sampling point—and unsampled. The relative proportions may transform under favorable hydrothermal conditions as $\text{Cl} + \text{Ca}^{2+} \leftrightarrow \text{Ep} + \text{Mg}^{2+}$ (Franz & Liebscher, 2004) and the calcium can be sourced from both the calcium minerals and the hot fluid. However, even if calcium minerals in fault rocks (granite and Gra) or injected water (Westaway & Burnside, 2019) can promote this transformation from Cl to Ep, which increases the possibility of fault instability and increases the seismic potential, whether this mechanism can explain the recent earthquake in Pohang merits further investigation. In natural granitoid fault zones and under high-grade greenschist metamorphic conditions ($T \sim 300^\circ\text{C} - 450^\circ\text{C}$), a much higher proportion of Ep is observed in the cataclasite, mylonite or ultramylonite than in the granitoid host (Sarkar et al., 2020; Wehrens et al., 2016). Such Ep-rich veins are the remnants of past injection cycles by overpressured thermal pore fluids and may be indicative of past paleoseismicity (Wehrens et al., 2016). The frictional response of Ep is therefore important in understanding the response of granitoid mylonites or ultramylonites in mid-crustal faults.

Ep and Cl are likely to be heterogeneously distributed within fault zones and along fracture planes since metamorphism results from interaction with heterogeneously distributed groundwaters (Samae et al., 2021; Spinelli & Wang, 2009). Rock cores sampled from 4.2 km in the Pohang geothermal reservoir (Kwon et al., 2019) indicate that the Pohang Gra is highly fractured—and correspondingly the fault zone is likely highly permeable (Caine et al., 1996). Thus, alteration and metasomatism would initially begin along the fluid pathway and progress outwards with the invasion of hydrothermal fluids from the fault. For the layered gouge, the phyllosilicate content has a critical effect on gouge friction and previous lab or modeling results showed that ~ 5 wt.% layered phyllosilicates can lower the frictional strength and stabilize the faults (Niemeijer et al., 2010; Wang et al., 2017). Such geometric constraints will apply to Cl/Ep mixtures when the layered Cl gouge is distributed within the layered Ep gouge—defining strength and stability as a function of mixture proportions and structure.

Our experimental results have implications for the generation of both natural and induced earthquakes in basement rocks, including for enhanced geothermal system and wastewater injection sites (Holdsworth et al., 2019; Trice et al., 2019). In EGS wells drilled for fluid injection may intersect critically-stressed fractures and fault zones (Figure 4). In such cases, the fault gouge zones control slip of the mature fault (Choi et al., 2016). If Ep is natively present in such regions and temperatures are in the range $150^\circ\text{C} - 250^\circ\text{C}$, our results suggest that friction will likely be velocity-weakening and therefore potentially unstable. Considering geothermal reservoirs with high thermal gradients ($40^\circ\text{C}/\text{km}$ or more) as representative, then temperatures at 4–5 km depth could be of the order $160^\circ\text{C} - 200^\circ\text{C}$ (Beckers et al., 2014; Olasolo et al., 2016) and the Ep gouge would then promote unstable sliding at both hydrostatic and elevated pore fluid pressures. Conversely, for faults containing Ep/Cl mixed gouges, a low Cl content can reduce fault frictional strength and promote failure but not necessarily unstable slip. Notably, low-grade metamorphism by epidotization and chloritization are also reported in the crystalline basement of northeastern Oklahoma and associated with the wastewater injection-triggered earthquakes (Hamilton et al., 2021; Kolawole et al., 2019)—where Ep veining in the Oklahoma basement exhibits velocity-weakening behavior at shallow depth (~ 3 km). Our results therefore imply a potential of fault instability by the presence of Ep and a potential for fault failure by the precipitation of Cl, allowing gouge composition to exert a subtle but significant control on fault strength and stability.

5. Conclusions

Our shear experiments on epidote or Ep/CL mixed gouges highlight their effect of alteration and metamorphism on the stability of subsurface faults in geothermal reservoirs. The results show that Cl-rich gouges exhibit much lower frictional strength than both the Pohang Gra and Ep-rich gouges at conditions typified by the typical geothermal reservoirs—implying that faults filled with Cl-rich gouges may be readily reactivated. On the other hand, the Gra gouges exhibit velocity-neutral to velocity-weakening behavior, in contrast to the Ep-rich gouges that show only frictional weakening at elevated temperatures and pore fluid pressures, promoting instability of subsurface faults and increasing their seismic potential. Our results demonstrate

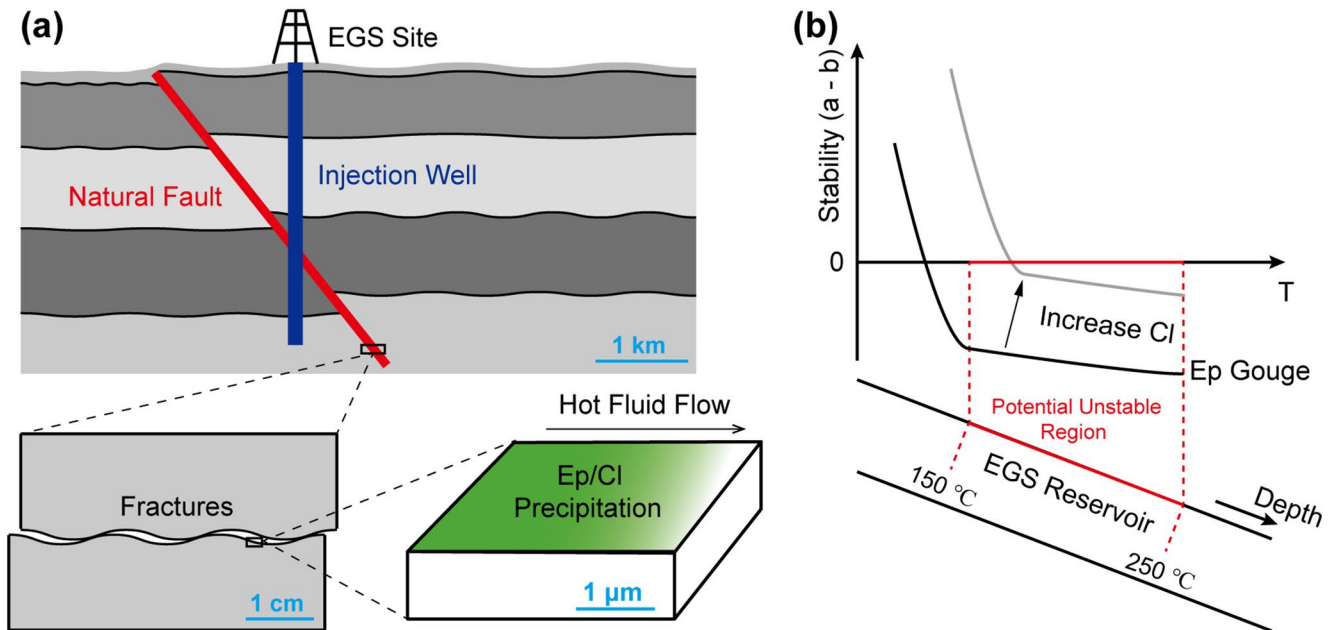


Figure 4. Interplay of the native presence of metamorphic minerals on fault stability at a typical enhanced geothermal system (EGS) site. (a) A drilled EGS well may transect the large-scale natural deep fault. Alteration minerals occur on the natural fault/fracture planes due to low-grade metamorphisms or interaction with subsurface hot fluid. (b) The temperature for an EGS reservoir generally spans the range of 150°C – 250°C (Olasolo et al., 2016). In this temperature range, fractures/faults altered or metamorphosed with epidote (Ep) or Ep-rich gouge exhibit velocity-weakening behavior and the potential for unstable reactivation. The areas surrounded by red lines or dashed lines indicate the potential unstable region of EGS reservoir metamorphosed by epidotization and chloritization.

that the presence of low-grade alterations or metamorphism should be taken into consideration in mitigating both natural and injection-induced seismic risks in such geologic environments.

Data Availability Statement

Raw data of all shear experiments are available at <https://doi.org/10.5061/dryad.0rxwdbx9>.

Acknowledgments

This work is supported by the National Key Research and Development Project (No. 2020YFC1808102) and National Natural Science Foundation of China (No. 41772286, 41941018, 42077247). The recovery of rock core from the Pohang EGS site was initially sponsored by a grant (No. 20123010110010) from the New and Renewable Energy Program of the Korea Institute of Energy Technology Evaluation and Planning, and funded by the Ministry of Trade, Industry and Energy of the Korean Government. XRD and microstructural characterization were conducted on natural granodiorite fractures recovered from Pohang Geothermal reservoir, and outcrop granite from Gonghe Geothermal site, China. We thank Jianye Chen and Xi Ma for laboratory assistance and Li Zhuang of the Korea Institute of Civil Engineering and Building Technology for providing the thin section from the Gonghe site. Comments by Juhyi Yim of Seoul National University is appreciated.

References

- Apted, M. J., & Liou, J. G. (1983). Phase relations among greenschist, epidote-amphibolite, and amphibolite in a basaltic system. *American Journal of Science*, 283(A), 328–354.
- Beckers, K. F., Lukowski, M. Z., Anderson, B. J., Moore, M. C., & Tester, J. W. (2014). Levelized costs of electricity and direct-use heat from enhanced geothermal systems. *Journal of Renewable and Sustainable Energy*, 6(1), 013141. <https://doi.org/10.1063/1.4865575>
- Bird, D. K., & Spieler, A. R. (2004). Epidote in geothermal systems. *Reviews in Mineralogy and Geochemistry*, 56, 235–300. <https://doi.org/10.2138/gsrmg.56.1.235>
- Blanpied, M. L., Lockner, D. A., & Byerlee, J. D. (1991). Fault stability inferred from granite sliding experiments at hydrothermal conditions. *Geophysical Research Letters*, 18(4), 609–612. <https://doi.org/10.1029/91GL00469>
- Bos, B., & Spiers, C. J. (2002). Frictional-viscous flow of phyllosilicate-bearing fault rock: Microphysical model and implications for crustal strength profiles. *Journal of Geophysical Research*, 107(B2), 2028. <https://doi.org/10.1029/2001jb000301>
- Caine, J. S., Evans, J. P., & Forster, C. B. (1996). Fault zone architecture and permeability structure. *Geology*, 24(11), 1025–1028. [https://doi.org/10.1130/0091-7613\(1996\)0242.3.CO;2](https://doi.org/10.1130/0091-7613(1996)0242.3.CO;2)
- Chen, J., Verberne, B. A., & Spiers, C. J. (2015). Effects of healing on the seismogenic potential of carbonate fault rocks: Experiments on samples from the Longmenshan Fault, Sichuan, China. *Journal of Geophysical Research: Solid Earth*, 120, 5479–5506. <https://doi.org/10.1002/2015JB012051>
- Choi, J. H., Edwards, P., Ko, K., & Kim, Y. S. (2016). Definition and classification of fault damage zones: A review and a new methodological approach. *Earth-Science Reviews*, 152, 70–87. <https://doi.org/10.1016/j.earscirev.2015.11.006>
- Den Hartog, S. A. M., & Spiers, C. J. (2013). Influence of subduction zone conditions and gouge composition on frictional slip stability of megathrust faults. *Tectonophysics*, 600, 75–90. <https://doi.org/10.1016/j.tecto.2012.11.006>
- Dieterich, J. H. (1979). Modeling of rock friction: 1. Experimental results and constitutive equations. *Journal of Geophysical Research*, 84(B5), 2161. <https://doi.org/10.1029/JB084iB05p02161>
- Ellsworth, W. L. (2013). Injection-induced earthquakes. *Science*, 341(6142), 1225942. <https://doi.org/10.1126/science.1225942>
- Evans, B. W. (1990). Phase relations of epidote-blueschists. *Lithos*, 25(1–3), 3–23. [https://doi.org/10.1016/0024-4937\(90\)90003-j](https://doi.org/10.1016/0024-4937(90)90003-j)

- Fagereng, Å., & Ikari, M. J. (2020). Low-temperature frictional characteristics of chlorite-epidote-amphibole assemblages: Implications for strength and seismic style of retrograde fault zones. *Journal of Geophysical Research: Solid Earth*, 125, e2020JB019487. <https://doi.org/10.1029/2020JB019487>
- Faulkner, D. R., Sanchez-Roa, C., Boulton, C., & den Hartog, S. A. M. (2018). Pore fluid pressure development in compacting fault gouge in theory, experiments, and nature. *Journal of Geophysical Research: Solid Earth*, 123(1), 226–241. <https://doi.org/10.1002/2017JB015130>
- Franz, G., & Liebscher, A. (2004). Physical and Chemical Properties of the Epidote Minerals—An Introduction. *Reviews in Mineralogy and Geochemistry*, 56(1), 1–81. <https://doi.org/10.2138/gsrng.56.1.1>
- Giorgetti, C., Carpenter, B. M., & Collettini, C. (2015). Frictional behavior of talc-calcite mixtures. *Journal of Geophysical Research: Solid Earth*, 120(9), 6614–6633. <https://doi.org/10.1002/2015JB011970>
- Grigoli, F., Cesca, S., Rinaldi, A. P., Manconi, A., López-Comino, J. A., Clinton, J. F., et al. (2018). The November 2017 M_w 5.5 Pohang earthquake: A possible case of induced seismicity in South Korea. *Science*, 360(6392), 1003–1006. <https://doi.org/10.1126/science.aat2010>
- Hamilton, M., Carpenter, B. M., Johnston, C. S., Evans, S. C., Elmore, R. D., & Elmore, R. D. (2021). Fractured, altered, and faulted basement in northeastern Oklahoma: Implications for induced seismicity. *Journal of Structural Geology*, 147, 104330. <https://doi.org/10.1016/j.jsg.2021.104330>
- He, C., Yao, W., Wang, Z., & Zhou, Y. (2006). Strength and stability of frictional sliding of gabbro gouge at elevated temperatures. *Tectonophysics*, 427(1–4), 217–229. <https://doi.org/10.1016/j.tecto.2006.05.023>
- Holdsworth, R. E., McCaffrey, K., Dempsey, E., Roberts, N., Robertson, A., Morton, A., et al. (2019). Natural fracture propping and earthquake-induced oil migration in fractured basement reservoirs. *Geology*, 47(8), 700–704. <https://doi.org/10.1130/G46280.1>
- Ikari, M. J., Marone, C., & Saffer, D. M. (2011). On the relation between fault strength and frictional stability. *Geology*, 39(1), 83–86. <https://doi.org/10.1130/G31416.1>
- Ikari, M. J., Saffer, D. M., & Marone, C. (2009). Frictional and hydrologic properties of clay-rich fault gouge. *Journal of Geophysical Research*, 114(B5), B05409. <https://doi.org/10.1029/2008JB006089>
- Kim, K. H., Ree, J. H., Kim, Y. H., Kim, S., Kang, S. Y., & Seo, W. (2018). Assessing whether the 2017 M_w 5.4 Pohang earthquake in South Korea was an induced event. *Science*, 360(6392), 1007–1009. <https://doi.org/10.1126/science.aat6081>
- Kolawole, F., Johnston, C., Morgan, B. C., Chang, J., Carpenter, B., Lockner, D. A., et al. (2019). The susceptibility of Oklahoma's basement to seismic reactivation. *Nature Geoscience*, 12(10), 839–844. <https://doi.org/10.1038/s41561-019-0440-5>
- Kovac, K. M., Moore, J. N., & Lutz, S. J. (2005). Geologic framework of the East Flank, Coso geothermal field: Implications for EGS Development. *Proceedings 30th Workshop on Geothermal Engineering* (p. 486). Stanford University:492.
- Kwon, S., Xie, L., Park, S., Kim, K. I., Min, K. B., Kim, K. Y., et al. (2019). Characterization of 4.2-km-deep fractured granodiorite cores from Pohang geothermal reservoir, Korea. *Rock Mechanics and Rock Engineering*, 52(3), 771–782. <https://doi.org/10.1007/s00603-018-1639-2>
- Lacroix, B., Charpentier, D., Buatier, M., Vennemann, T., Labaume, P., Adatte, T., et al. (2012). Formation of chlorite during thrust fault reactivation. Record of fluid origin and P-T conditions in the Monte Perdido thrust fault (southern Pyrenees). *Contributions to Mineralogy and Petrology*, 163(6), 1083–1102. <https://doi.org/10.1007/s00410-011-0718-0>
- Lee, K.-K., Ellsworth, W. L., Giardini, D., Townend, J., Ge, S., Shimamoto, T., et al. (2019). Managing injection-induced seismic risks. *Science*, 364(6442), 730–732. <https://doi.org/10.1126/science.aax1878>
- Lee, K.-K., Yeo, I.-W., Lee, J.-Y., Kang, T.-S., Rhie, J., Sheen, D.-H., et al. (2019). *Summary report of the Korean Government commission on relations between the 2017 Pohang earthquake and EGS Project*. In Geological Society of Korea and Korean Government Commission on the Cause of the Pohang Earthquake. Retrieved from http://www.gskorea.or.kr/custom/27/data/Summary_Report_on_Pohang_Earthquake_March_20_2019.pdf
- Logan, J. M., Dengo, C. A., Higgs, N. G., & Wang, Z. Z. (1992). Fabrics of experimental fault zones: Their development and relationship to mechanical behavior. In B. Evans, & T.-F. Wong (Eds.), *Fault mechanics and transport properties of rocks* (pp. 33–67). Academic Press. [https://doi.org/10.1016/S0074-6142\(08\)62814-4](https://doi.org/10.1016/S0074-6142(08)62814-4)
- Majer, E. L., Baria, R., Stark, M., Oates, S., Bommer, J., Smith, B., & Asanuma, H. (2007). Induced seismicity associated with enhanced geothermal systems. *Geothermics*, 36(3), 185–222. <https://doi.org/10.1016/j.geothermics.2007.03.003>
- Marone, C. (1998). Laboratory-derived friction laws and their application to seismic faulting. *Annual Review of Earth and Planetary Sciences*, 26(1), 643–696. <https://doi.org/10.1146/annurev.earth.26.1.643>
- Niemeijer, A., Marone, C., & Ellsworth, D. (2010). Fabric induced weakness of tectonic faults. *Geophysical Research Letters*, 37(3), L03304. <https://doi.org/10.1029/2009GL041689>
- Niemeijer, A. R., & Collettini, C. (2014). Frictional properties of a low-angle normal fault under in situ conditions: Thermally-activated velocity weakening. *Pure and Applied Geophysics*, 171(10), 2641–2664. <https://doi.org/10.1007/s00024-013-0759-6>
- Okamoto, A. S., Verberne, B. A., Niemeijer, A. R., Takahashi, M., Shimizu, I., Ueda, T., & Spiers, C. J. (2019). Frictional properties of simulated chlorite gouge at hydrothermal conditions: Implications for subduction megathrusts. *Journal of Geophysical Research: Solid Earth*, 124(5), 4545–4565. <https://doi.org/10.1029/2018JB017205>
- Olasolo, P., Juárez, M. C., Morales, M. P., Damico, S., & Liarte, I. A. (2016). Enhanced geothermal systems (EGS): A review. *Renewable and Sustainable Energy Reviews*, 56, 133–144. <https://doi.org/10.1016/j.rser.2015.11.031>
- Poli, S., & Schmidt, M. W. (2004). Experimental subsolidus studies on epidote minerals. *Reviews in Mineralogy and Geochemistry*, 56, 171–195. <https://doi.org/10.2138/gsrng.56.1.171>
- Rice, J. R. (1983). Constitutive relations for fault slip and earthquake instabilities. *Pure and Applied Geophysics*, 121(3), 443–475. <https://doi.org/10.1007/BF02590151>
- Ruina, A. (1983). Slip instability and state variable friction laws. *Journal of Geophysical Research*, 88(B12), 10359–10370. <https://doi.org/10.1029/JB088iB12p10359>
- Samae, V., Cordier, P., Demouchy, S., Bollinger, C., Gasc, J., Koizumi, S., et al. (2021). Stress-induced amorphization triggers deformation in the lithospheric mantle. *Nature*, 591, 82–86. <https://doi.org/10.1038/s41586-021-03238-3>
- Sarkar, G., Banerjee, S., Maity, S., & Srivastava, H. B. (2020). Fluid assisted rejuvenation of precursor brittle fractures as the habitats of ductile shear zones: An example from the ~2.6 Ga Bundelkhand Granitoid of north-central India. *Journal of Structural Geology*, 141, 104198. <https://doi.org/10.1016/j.jsg.2020.104198>
- Schleicher, A. M., van der Pluijm, B. A., & Warr, L. N. (2012). Chlorite-smectite clay minerals and fault behavior: New evidence from the San Andreas Fault Observatory at Depth (SAFOD) core. *Lithosphere*, 4(3), 209–220. <https://doi.org/10.1130/L158.1>
- Sonnenenthal, E., Spycher, N., Callahan, O., Cladouhos, T., & Petty, S. (2012). A thermal-hydrological-chemical model for the enhanced geothermal system demonstration project at Newberry Volcano, Oregon. In *Proceedings of the 37th workshop on G. eothermal Reservoir Engineering*.

- Spinelli, G. A., & Wang, K. (2009). Links between fluid circulation, temperature, and metamorphism in subducting slabs. *Geophysical Research Letters*, 36(13), L13302. <https://doi.org/10.1029/2009GL038706>
- Tembe, S., Lockner, D. A., & Wong, T.-F. (2010). Effect of clay content and mineralogy on frictional sliding behavior of simulated gouges: Binary and ternary mixtures of quartz, illite, and montmorillonite. *Journal of Geophysical Research*, 115, B03416. <https://doi.org/10.1029/2009JB006383>
- Trice, R., Hiorth, C., & Holdsworth, R. (2019). Fractured basement play development on the UK and Norwegian rifted margins. *Geological Society of London*. <https://doi.org/10.1144/SP495-2018-174>
- Verberne, B. A., He, C., & Spiers, C. J. (2010). Frictional properties of sedimentary rocks and natural fault gouge from the Longmenshan fault zone, Sichuan, China. *Bulletin of the Seismological Society of America*, 100(5B), 2767–2790. <https://doi.org/10.1785/0120090287>
- Verberne, B. A., Niemeijer, A. R., Bresser, J. D., & Spiers, C. J. (2015). Mechanical behavior and microstructure of simulated calcite fault gouge sheared at 20–600°C: Implications for natural faults in limestones. *Journal of Geophysical Research Solid Earth*, 120(12), 8169–8196. <https://doi.org/10.1002/2015JB012292>
- Vidal, J., & Genter, A. (2018). Overview of naturally permeable fractured reservoirs in the central and southern Upper Rhine Graben: Insights from geothermal wells. *Geothermics*, 74, 57–73. <https://doi.org/10.1016/j.geothermics.2018.02.003>
- Wang, C., Elsworth, D., & Fang, Y. (2017). Influence of weakening minerals on ensemble strength and slip stability of faults. *Journal of Geophysical Research: Solid Earth*, 122(9), 7090–7110. <https://doi.org/10.1002/2016JB013687>
- Wehrens, P., Berger, A., Peters, M., Spillmann, T., & Herwegh, M. (2016). Deformation at the frictional-viscous transition: Evidence for cycles of fluid-assisted embrittlement and ductile deformation in the granitoid crust. *Tectonophysics*, 693, 66–84. <https://doi.org/10.1016/j.tecto.2016.10.022>
- Westaway, R., & Burnside, N. M. (2019). Fault “corrosion” by fluid injection: A potential cause of the November 2017 M_w 5.5 Korean Earthquake. *Geofluids*, 2019, 1–23. <https://doi.org/10.1155/2019/1280721>
- Wojatschke, J., Scuderi, M. M., Warr, L. N., Carpenter, B. M., Saffer, D., & Marone, C. (2016). Experimental constraints on the relationship between clay abundance, clay fabric, and frictional behavior for the Central Deforming Zone of the San Andreas Fault. *Geochemistry, Geophysics, Geosystems*, 17, 3865–3881. <https://doi.org/10.1002/2016GC006500>